

# The Alzheimer-like phosphorylation of tau protein reduces microtubule binding and involves Ser-Pro and Thr-Pro motifs

N. Gustke<sup>a</sup>, B. Steiner<sup>a</sup>, E.-M. Mandelkow<sup>a</sup>, J. Biernat<sup>a</sup>, H.E. Meyer<sup>b</sup>, M. Goedert<sup>c</sup> and E. Mandelkow<sup>a</sup>

<sup>a</sup>Max-Planck-Unit for Structural Molecular Biology, c/o DESY, Notkestraße 85, D-2000 Hamburg 52, Germany, <sup>b</sup>Institut für Physiologische Chemie, Ruhr-Universität Bochum, Universitätsstr. 150, Geb. MA2/143, D-4630 Bochum, Germany and <sup>c</sup>MRC Laboratory of Molecular Biology, Hills Road, Cambridge CB2 2QH, UK

Received 27 May 1992; revised version received 5 June 1992

Tau protein can be transformed into an Alzheimer-like state by phosphorylation with a kinase activity from brain [Biernat et al. (1992) EMBO J. 11, 1593–1597]. Here we show that the phosphorylation at Ser-Pro motifs strongly decreases tau's affinity for microtubules. The major reduction occurs during the first of the three main stages of phosphorylation. The data explain the lower stability of microtubules resulting from the pathological tau phosphorylation.

Tau protein; Microtubule; Alzheimer's disease; Phosphorylation; Proline-directed kinase

## 1. INTRODUCTION

Neurofibrillary tangles constitute one of the characteristics of Alzheimer's disease. They are correlated with the presence and severity of dementia, and their distribution permits a neuropathological distinction between preclinical and clinical cases [4]. Their main components are the paired helical filaments (PHFs) which consist of the microtubule-associated protein tau [11,25]. Tau proteins are a group of developmentally regulated nervous system proteins that promote microtubule assembly and stability [7]; they are generated from a single gene by alternative mRNA splicing [11,12,17,24]. In human brain this generates a total of six related isoforms. They differ from each other by the presence of three or four microtubule-binding domains located in the C-terminal half and by the presence or absence of 29 or 58 amino acid insertions located near the N terminus [12].

When run on SDS gels the PHFs produce several modified tau bands as their major components [14,23,25]. These bands show a reduced gel mobility and consist of abnormally phosphorylated tau. The use of anti-tau antibodies whose staining of neurofibrillary tangles and PHF tau bands is phosphorylation-dependent has indicated the existence of several sites that may be abnormally phosphorylated [5,15,21,32].

It has been conjectured that the aberrant phosphorylation of tau leads to its dissociation from microtubules and to its aggregation into PHFs and that the ensuing

destabilization of microtubules causes the degeneration of the affected nerve cells (reviewed in [13,22]). We have recently found a protein kinase activity in adult pig brain which induces a PHF-like state in normal or recombinant tau proteins, as judged by a reduced gel mobility and the reaction with PHF tau-specific antibodies [3,26]. In this report we describe how the kinase reduces the tau-microtubule interaction. The most conspicuous effect is that the stoichiometry of tau to tubulin decreases 3-fold or more. The phosphorylation occurs mainly at Ser-Pro or Thr-Pro motifs.

## 2. MATERIALS AND METHODS

The methods for tau preparation, phosphorylation, and analysis of phosphorylation sites have been described previously. Briefly, recombinant human tau proteins (derived from the cDNA clones of Goedert et al., [12]) were expressed in *E. coli* and prepared as described [16,30]. Point mutants were made by PCR, and phosphorylation by the brain kinase was done following [3]. The protein was dialyzed against reassembly buffer (RB, 100 mM Na-PIPES pH 6.9, 1 mM EGTA, 1 mM GTP, 1 mM MgSO<sub>4</sub>, 1 mM DTT) and used for binding studies (see below). Radioactive labeling was done with [ $\gamma$ -<sup>32</sup>P]ATP (NEN Du Pont) at 10 mCi/ml, radioactive tryptic peptides were generated, isolated by HPLC, and sequenced as described [3,30]. For details on sequencing methods see [8,29].

### 2.1. Binding studies

Tubulin purified by MAP-depleting steps and phosphocellulose chromatography [28] was incubated at 37°C in the presence of 1 mM GTP and 20  $\mu$ M taxol. After 10 min tau protein was added in different concentrations and incubated for another 10 min. The suspensions were centrifuged for 35 min at 43,000  $\times$  g at 37°C. The resulting pellets were resuspended in CB buffer (50 mM PIPES pH 6.9, 1 mM EGTA, 0.2 mM MgCl<sub>2</sub>, 5 mM DTT, 500 mM NaCl). In the case of htau23 and htau34 the pellets and supernatants were boiled for 10 min and recentrifuged for 10 min at 43,000  $\times$  g at 4°C (this step served to

Correspondence address: E. Mandelkow, Max-Planck-Unit for Structural Molecular Biology, c/o DESY, Notkestraße 85, D-2000 Hamburg 52, Germany. Fax: (49) (40) 891314.

remove the tubulin component which otherwise would overlap with these tau isoforms on SDS gels). Pellets and supernatants (containing the bound and the free tau, respectively) were subjected to SDS PAGE (gradient 7–15% acrylamide) and stained with Coomassie brilliant blue R250. The gels were scanned at 400 dpi on an Epson GT 6000 scanner and evaluated on a PC 386AT using the program GelScan (G. Spieker, Aachen). The protein concentration on the gel was always within the linear range (up to 1.5 optical density units). The intensities were transformed to concentrations using calibration curves and used in the binding equation

$$\text{Tau}_{\text{bound}} = n[\text{Mt}][\text{Tau}_{\text{free}}] / \{K_d + [\text{Tau}_{\text{free}}]\},$$

from which the dissociation constant  $K_d$  and the number  $n$  of binding sites per dimer were obtained by curve fitting.  $[\text{Mt}]$  is the concentration of tubulin dimers polymerized in microtubules (usually  $30 \mu\text{M}$ ). SDS-PAGE was done with gradients of 4–20% or 7–15%.

### 3. RESULTS

A characteristic feature of the kinase activity is that it shifts the  $M_r$  of all tau isoforms in three distinct stages (see Fig. 1a for the case of htau23). During the first 2 h of phosphorylation the protein is converted from a  $M_{r0} = 48 \text{ kDa}$  protein to a slower species, with an  $M_{r1}$  of about  $52 \text{ kDa}$ . Upon completion of this first stage, a second one sets in which is finished around 6–10 h ( $M_{r2} = 54 \text{ kDa}$ ). The third stage takes about 24 h ( $M_{r3} = 56 \text{ kDa}$ ), after which no more shift is observed.

The autoradiogram (Fig. 1b) confirms the progressive incorporation of phosphate. By quantitation of the bands we found that after 24 h there is a maximum of 5–6 phosphates (6–7 in the case of htau34, see below). This end point is not limited by ATP; it could be due to a decay of the kinase activity, or to a saturation of the phosphorylatable sites. The extent of phosphorylation depends on the level of okadaic acid (OA), a phosphatase inhibitor [2]. 1 nM OA has no effect, implying that PPase-2A does not operate on tau. However,  $10 \mu\text{M}$  OA induces clear differences (Fig. 1b, compare even and odd lanes); without it the phosphorylation is  $\approx 1$ –2  $P_i$  less than the maximum. This implies that PPase-1 is responsible for the difference (since PPase-2B/calciueurin was inhibited by 5 mM EGTA in both experiments). Without EGTA there is only minor phosphorylation of Ser-Pro motifs, and preliminary results show that this is due to dephosphorylation by calcineurin (unpublished).

During the initial stage each band of the tau doublet incorporates phosphate (e.g. at a level of about one  $P_i$  per molecule in the presence of OA at 30 min, see Fig. 1b, lane 4). This means that there must be two distinct types of phosphorylation sites, one that is responsible for the shift (the 'shift site', upper band), and one that has no effect on the  $M_r$  (lower band). The lower band gradually disappears, and at two hours each tau molecule contains about 2  $P_i$ . The upper band thus contains tau molecules in which the 'shift site' is phosphorylated whereas the lower band contains only molecules where

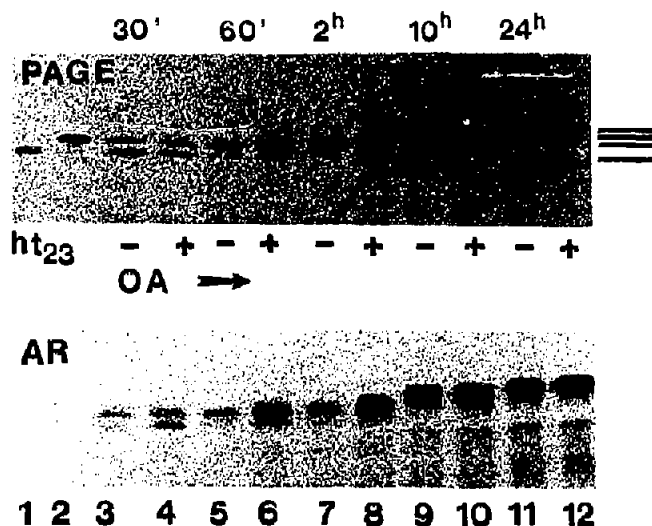


Fig. 1. Time course of phosphorylation of bacterially expressed human isoform htau23 with the brain kinase activity and corresponding autoradiogram. (a) SDS-PAGE of htau23 after incubation with the kinase activity between 0 and 24 h, as indicated. The unphosphorylated protein is a single band of  $M_{r0} = 48 \text{ kDa}$  (lane 1). Lanes 3–14 show that phosphorylation leads to stepwise shifts to higher  $M_r$ , with well defined intermediate stages. The even lanes (numbered 4, 6, etc. below Fig. 1b) are observed in the presence of  $10 \mu\text{M}$  okadaic acid (labeled '+' below Fig. 1a). The odd lanes (3, 5, etc., labeled '-') are without okadaic acid. The first stage takes about 2 h (shift to a new  $M_{r1} = 52 \text{ kDa}$ ), the second is finished around 10 h ( $M_{r2} = 54 \text{ kDa}$ ), the third is finished around time 24 h ( $M_{r3} = 56 \text{ kDa}$ ); no further shift is observed during the subsequent 24 h. Lane 2 shows a mutant where Ser-404 was replaced by Asp; note that the  $M_r$  shift is similar to the top band of lane 3. The  $M_r$  shifts corresponding to the main stages of phosphorylation are shown on the right. (b) Autoradiogram of (a). The quantitation of the phosphate incorporated (mol  $P_i$ /mol protein) in this experiment was as follows (–OA/+OA): 30 min (0.5/1.0), 60 min (0.7/1.4), 120 min (1.0/2.0), 10 h (2.0/3.0), 24 h (3.2/4.0). The final values in this experiment are lower than the maximum of 5–6 found with htau23.

the shift site is not phosphorylated. The effect of OA is seen mainly in the lower band, indicating that the phosphatase operates mainly on the non-shift site(s). These considerations apply to the first stage of phosphorylation; during the second and third stages there are further shifts (substages), but a detailed analysis is not possible because of the overlap of bands.

In order to clarify the relationship between phosphorylation and microtubule binding we determined the phosphorylated residues. The  $^{32}\text{P}$ -phosphorylated protein was digested with trypsin (Fig. 2a), the main radioactive peptides (Fig. 2b) were separated by HPLC (Fig. 2c), and the phosphorylated residues were determined by gas phase sequencing (for methods see [29]). The sites phosphorylated at stage 3 are summarized in Table I. They include serines 46, 199, 202, 235, 396, 404, 422 (Fig. 3). These serines are conserved among all human tau isoforms, except Ser-46 which lies in the first N-terminal insert and is absent in htau23 and htau24. All of these serines are followed by prolines, and all Ser-Pro motifs were phosphorylated. Several of these

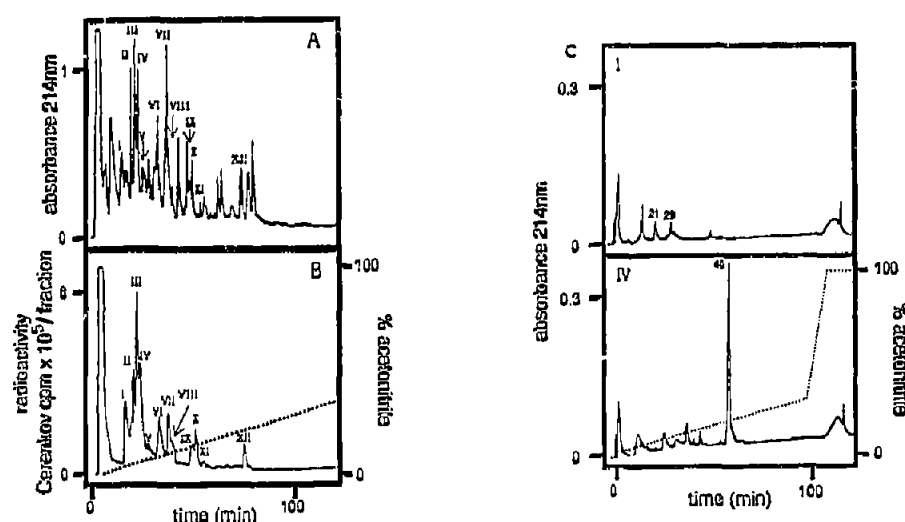


Fig. 2. Separation and identification of tryptic phosphopeptides on first HPLC gradient. The example shows a sample of 20 nmol of htau34 phosphorylated for 24 h with brain extract. (a) Peptide profile of gradient, measured by absorbance at 214 nm. Roman numerals (arrows) indicate the radioactive peaks, see (b). (b) Radioactivity profile of the gradient, obtained by measuring the individual fractions (0.5 ml) in Cerenkov mode in a liquid scintillation counter. The dotted line shows the acetonitrile gradient. (c) Examples of the final purification of radioactive peptides on the second HPLC gradient for subsequent sequencing. Top, peak I from first HPLC column, with radioactive fraction I-21 and I-29. Bottom, peak IV, radioactive fraction IV-48. See Table I for sequence of peptides.

serines form part of phosphorylation sensitive epitopes of antibodies that distinguish between normal and PHF tau [3,25,26]. The sites are clustered around residue 200 (just before the internal repeats) and around residue 400 (after the repeats). Thus most sites are in the assembly domain (Ser-199–Leu-441) and flank the repeat region. In addition to the sites described above the fully phosphorylated protein also contained some other sites such as serines 262 and 356, and two threonines, 181 and 212, both followed by prolines. However, Ser-416, the target of the CaM kinase we determined previously [30] was not phosphorylated.

Next we investigated whether the phosphorylation by the kinase activity had an influence on the binding of tau to microtubules. This was done by quantifying how

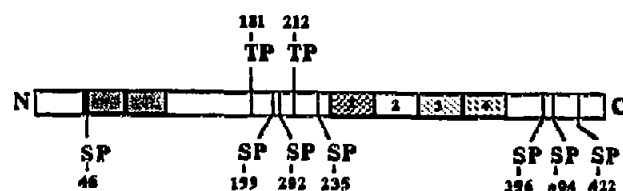


Fig. 3. Bar diagram of htau40, showing the location of the 7 Ser-Pro motifs phosphorylated by the kinase activity. The boxes labeled 1–4 are the internal repeats involved in microtubule binding; the second is absent in some isoforms (e.g. htau23). The two shaded boxes near the N terminus are inserts absent in htau23 and htau24 so that these molecules have only 6 Ser-Pro motifs.

Table I  
Sequences of phosphorylated peptides

Peak, Fraction	Peptide	Phosphorylated amino acid
I-21	231 TPPKS <sub>p</sub> PSSAK	Ser-235
I-29	195 SGYSS <sub>p</sub> PGS <sub>p</sub> PGT...	Ser-199 and -202
II-32	195 SGYSS <sub>p</sub> PGS <sub>p</sub> PG...	Ser-199 and -202
II-34	396 SPVVS <sub>p</sub> GDT <sub>p</sub> PR	Ser-404
III-21	231 TPPKS <sub>p</sub> PSSAK	Ser-235
III-34	260 IGS <sub>p</sub> TENLK	Ser-262
IV-48	25 DQGGYTMHQDQEGD <sub>p</sub> TAGLKES <sub>p</sub> PLQ...	Ser-46
VI-35	175 TPPAKT <sub>p</sub> PPSSGEP <sub>p</sub> PK	Thr-181
VI-46	384 AKTDHGAEIVYKS <sub>p</sub> PVVS <sub>p</sub> GDT...	Ser-396
VII-51	384 AKTDHGAEIVYKS <sub>p</sub> PVVS <sub>p</sub> GDT <sub>p</sub> PR	Ser-396 and -404
VIII-47	384 AKTDHGAEIVYKS <sub>p</sub> PVVS <sub>p</sub> GDT...	Ser-396
IX-54	354 IGS <sub>p</sub> LDNITHVPGGQNK	Ser-356
X-46	210 SRT <sub>p</sub> PSLPTPTREPK	Thr-212
XII-83	407 HLSNVSS <sub>p</sub> TGSIDMVDS <sub>p</sub> PQLATL...	Ser-422

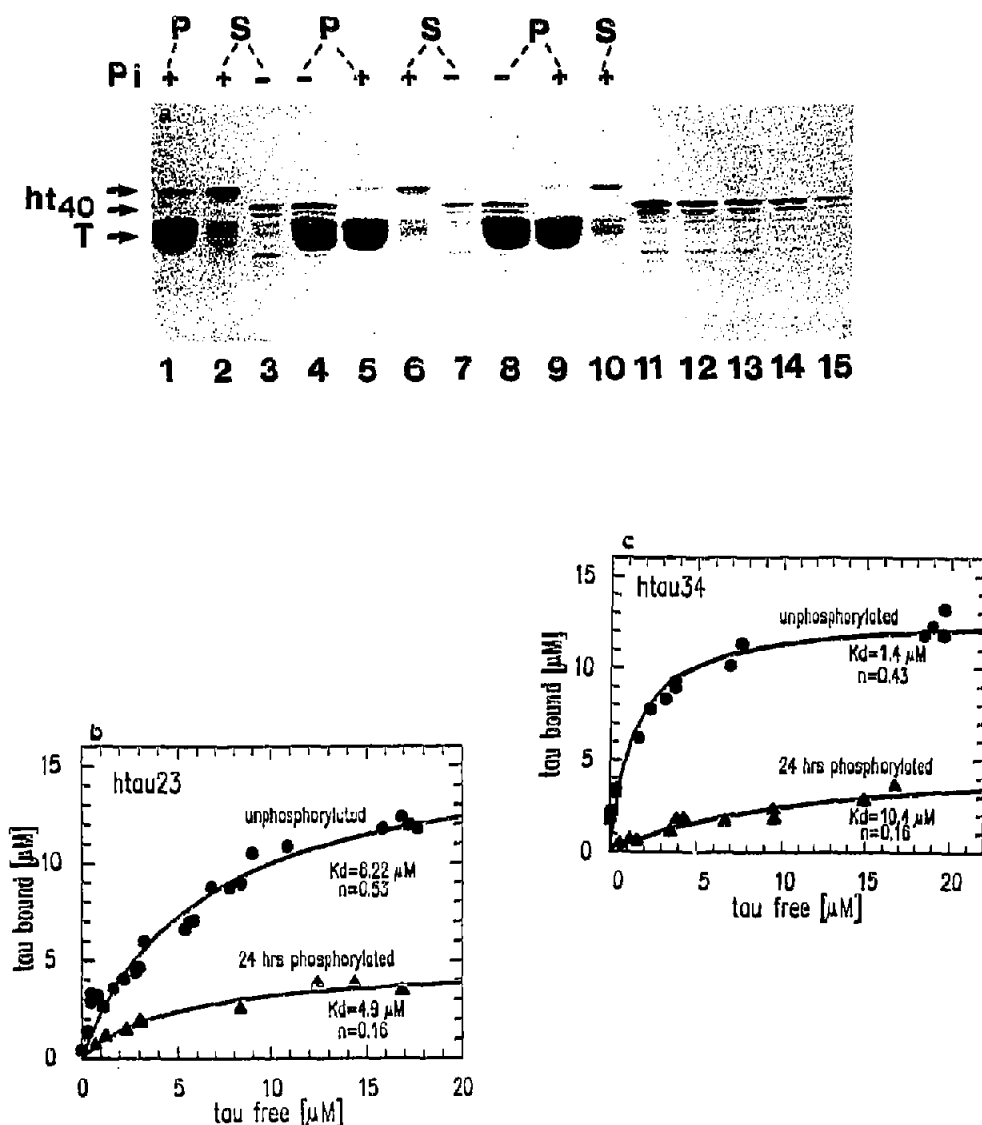


Fig. 4. Binding of tau isoforms to microtubules before and after phosphorylation. (a) SDS gel of a binding experiment, illustrated for the case of the tau isoform ht40 (whose band is clearly separated from that of tubulin (T) so that both components can be shown simultaneously, without having to remove tubulin by a boiling step, see section 2. The top line indicates pellets (P) or supernatants (S), with or without phosphorylation for 24 h (+ or -P). Lanes 1-4, 20  $\mu$ M tau protein (total concentration), phosphorylated (lanes 1, 2) or not (lanes 3, 4). The comparison of lanes 1 and 2 shows that most of the phosphorylated protein is free (S), while only a small fraction is bound to the microtubules (P). Lanes 3 and 4 show that in the unphosphorylated state about half of the protein is bound, the other half free (note also that the phosphorylated protein bands, lanes 1, 2, are higher in the gel than the unphosphorylated ones, lanes 3, 4, similar to Fig. 1). Lanes 5-8, similar experiment with 15  $\mu$ M ht40. Lanes 9, 10 show the case of 10  $\mu$ M phosphorylated protein. Lanes 11-15 are for density calibration with known amounts of ht40 (15, 10, 7.5, 5, and 2.5  $\mu$ M, respectively). (b) Binding curves of ht23 and (c) ht34 to microtubules before (circles) and after 24 h phosphorylation (triangles); these curves were derived from SDS gels similar to that of Fig. 4a. Polymerized tubulin is 30  $\mu$ M. Fitted dissociation constants  $K_d$  and stoichiometries are as indicated. In each case the most dramatic effect is on the number of binding sites which decrease about three-fold upon phosphorylation, from around 0.5 (i.e. one tau for every two tubulin dimers) down to about 0.16 (one tau for six tubulin dimers). Note that the binding of unphosphorylated 4-repeat isoforms (such as ht34) is particularly high ( $K_d$  around 1-2  $\mu$ M).

much tau attached to taxol-stabilized microtubules (Fig. 4a). With fully phosphorylated protein (stage 3, 24 h) we observed a dramatic decrease in binding capacity of ht23 (Fig. 4b), from about one tau per two tubulin dimers to one tau per six tubulin dimers. In other words, it appears that unphosphorylated tau packs densely onto a microtubule surface, whereas fully phos-

phorylated tau behaves as if it covered the microtubule surface less densely and occupied more space. Fig. 4c shows the same experiment with ht34. The results are similar, i.e. there is a threefold reduction in binding capacity. We also note that tau isoforms with four repeats, such as ht34, bind to microtubules particularly tightly in the unphosphorylated state ( $K_d \approx 1-2 \mu$ M).

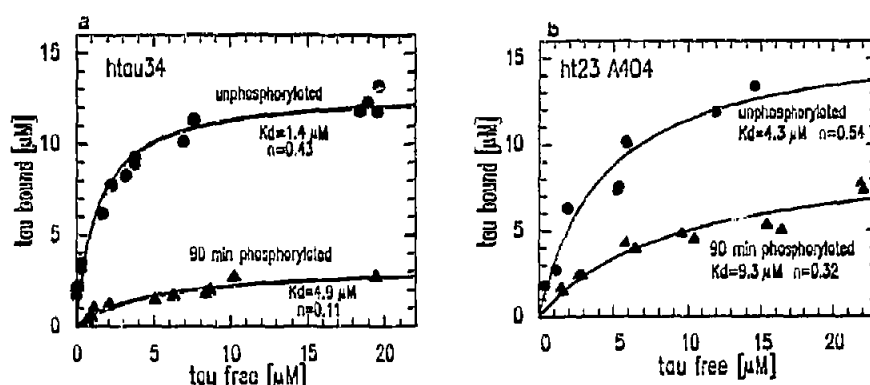


Fig. 5. (a) Binding of htau34 to microtubules, before (circles) and after phosphorylation for 90 min (stage 1, triangles). The reduction in binding capacity is very similar to that after 24 h phosphorylation (compare Fig. 4c). (b) Binding of ht23 (Ser-404→Ala) to microtubules, before (circles) and after 90 min phosphorylation (triangles). The unphosphorylated protein has similar binding characteristics as its parent molecule (Fig. 4b); the phosphorylated protein shows a reduction in binding capacity, but the effect is not as pronounced as with the parent protein.

Since the major  $M_r$  shift occurs during the initial two hours we investigated which residues become phosphorylated during this first stage, and how this affects microtubule binding. As mentioned above (Fig. 1), there are about two phosphates incorporated during this period, one of which causes the shift from  $M_{r0}$  to  $M_{r1}$ . Fig. 5a illustrates the binding of htau34 to microtubules after 90 min of phosphorylation. The striking result is that the limited phosphorylation decreases the affinity as efficiently as the full phosphorylation.

The analysis of tryptic peptides after 90 min (stage 1) showed four major peaks of radioactivity, with phosphates on serines 202, 235, 404, and 262. The first three are Ser-Pro sites that are not in the repeat region, but rather flank that region in nearly symmetric positions (Fig. 3). The fourth (Ser-262) is a non-Ser-Pro site in the first repeat. We made several point mutants to find out which site(s) were responsible for the initial  $M_r$  shift. When serine 404 was turned into alanine the  $M_r$  shift

during the first stage disappeared (Fig. 6a), whereas it remained visible when serines 199, 202, 235, or 396 were mutated. This means that the phosphorylation of serine 404 accounts for the one  $P_i$  present in the upper band of the first shift in Fig. 1a. The additional  $\approx 1 P_i$  present after 2 h is distributed among serines 202, 235, and 262.

These results suggest that the  $M_r$  of tau is particularly sensitive to certain phosphorylation sites downstream of the repeat region. We compared the gel shifts obtained by phosphorylating Ser-416 (the CaM kinase site) and the Ser-404 site (Fig. 6b, lanes 1–3). Note that phosphorylated Ser-404 has a larger effect than Ser-416; in both cases it is remarkable that a single phosphate induces the pronounced effect. A similar shift can be obtained by replacing Ser-404 with Asp (Fig. 1a, lane 2). At later stages the incorporation of more phosphates shifts the  $M_r$  even higher, up to the final value at 24 h (Fig. 6b, lanes 4, 5).

Whereas the results on the 'shift site' Ser-404 of tau

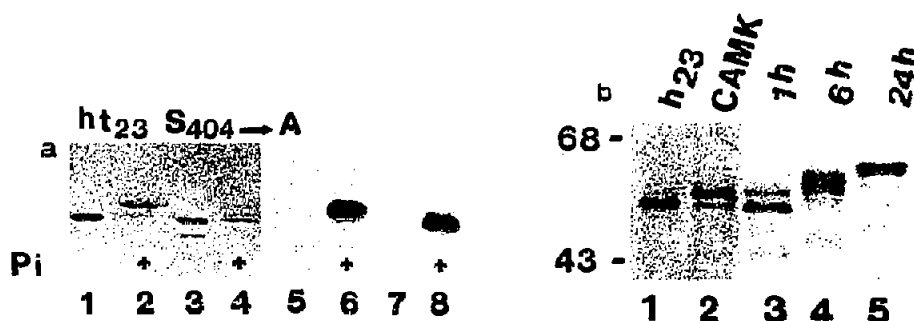


Fig. 6. Effects of point mutations of ht23 on  $M_r$  shift. (a) SDS gel of ht23 and the point mutant Ser-404→Ala, before and after 90 min phosphorylation. Lanes 1 and 2, ht23 before and after phosphorylation. Lanes 3 and 4, ht23/Ser-404→Ala mutant before and after phosphorylation. Lanes 5–8, autoradiogram of lanes 1–4. Note that both proteins are phosphorylated, but only ht23 shows the  $M_r$  shift. (b) SDS gel shifts of tau in different states of phosphorylation. Molecular weight markers are given on the left. Lane 1, ht23, unphosphorylated; lane 2, ht23, phosphorylated with  $Ca^{2+}$ -calmodulin-dependent kinase II (phosphorylating Ser-416 in ht40 numbering, [30]). Only part of the protein is phosphorylated so that the unshifted and shifted protein give rise to two bands; lanes 3–5, ht23 phosphorylated with kinase activity from brain extract for 1, 6, and 24 h, respectively. In lane 3 (stage 1 phosphorylation) only part of the protein is shifted up, similar to lane 2, but note the larger spacing between the bands. Lane 4 corresponds to stage 2 which actually comprises several substages (3–4 bands are visible). Lane 5 shows the final stage 3 with the largest shift.

are clear cut, the factors responsible for the reduction in microtubule binding are more complex. The Ser-404→Ala mutant binds to microtubules similarly as the parent tau23; after 90 min of phosphorylation the stoichiometry decreases about 2-fold, i.e. less than the factor of 3 observed with the parent molecule (Fig. 5b). If Ser-404 were the only residue whose phosphorylation was responsible for the loss of microtubule binding we would not expect any decrease in the mutant. The fact that a decrease is observed means that additional factors play a role; these are presumably related to the incorporation of more than one P<sub>i</sub> at one or more of the other sites before or at the beginning of the repeat region (e.g. Ser-202, Ser-235, Ser-262). However, these residues cannot by themselves be responsible for the full decrease of affinity either. In fact, point mutations at positions Ser-202 or Ser-235 show a similar effect as that of Ser-404, i.e. only a partial reduction of binding. One possible explanation is that different phosphorylation sites interact in a cooperative manner and generate a new conformation.

#### 4. DISCUSSION

The death of neurons in Alzheimer's disease may be due to several causes. Two possible factors may be suggested on the basis of the PHF pathology. One is the clogging of the somatodendritic compartment by the insoluble PHFs, the other is the destabilization of microtubules resulting from abnormal tau phosphorylation. We have recently identified a protein kinase activity in brain and a phosphorylation state of tau protein that resembles the state in Alzheimer PHFs in two ways: It has a reduced mobility in SDS gels, and it is recognized by PHF-specific antibodies [3,26]. It therefore became important to determine whether this state of tau also had a reduced interaction with microtubules. In this report we show that this is indeed the case.

Each stage of phosphorylation leads to an upward  $M_r$  shift of tau (Fig. 1). A threefold reduction in the binding of tau to microtubules occurs during the first stage (Fig. 4). By contrast, the reactivity of tau with the PHF tau-specific antibodies sets in only during the second stage. The kinase activity is dominated by a Ser-Pro-directed kinase (mainly MAP kinase [33]). At 24 h all Ser-Pro sites of tau have become phosphorylated (6 or 7, depending on the isoform). Two phosphates are incorporated during the first stage, and the one that accounts for the clear shift in  $M_r$  is at Ser-404 (Fig. 6). The other sites phosphorylated during the first stage are Ser-202, Ser-235, and Ser-262 (one of the non-Ser-Pro sites); they account for the second phosphate incorporated. These residues are distinct from two phosphorylation sites described previously. Ser-396, at the center of a Lys-Ser-Pro motif located after the tandem repeat region, is abnormally phosphorylated in PHF tau [25]; under the present assay conditions this site is only phosphorylated

during stages 2 and 3 and can thus not be responsible by itself for the first  $M_r$  shift or the reduction in microtubule binding. We had previously identified Ser-416 as the only residue phosphorylated by CaM kinase in recombinant tau [30]; this site was not phosphorylated under the conditions used here. Moreover, phosphorylation of this site does not result in PHF tau-like immunoreactivity with the SMI antibodies or in a reduction in microtubule binding. The single CaMK site does lead to a clear gel shift, but its magnitude is somewhat less than that caused by phosphorylation at Ser-404 (Fig. 6b). Note that the mutation Ser-404→Asp leads to a similar shift as phosphorylation at Ser-404. This means that the introduction of negative charges in the region of residue 400 tends to yield a shift in  $M_r$ , but on the other hand the occurrence of a shift does not necessarily imply a PHF-like phosphorylation (as is sometimes assumed).

The recombinant tau proteins bind to microtubules with dissociation constants of a few  $\mu$ M, and with stoichiometries around 0.5, i.e. one tau molecule for about two tubulin dimers in a microtubule (Fig. 4). The  $K_d$  values are comparable with those seen by others if one makes some allowance for the differences in protein type and preparation [6,7,9], but the stoichiometries are remarkably high compared to those of tau from brain tissue (around 0.2 or less, see [7,18]). When recombinant tau is phosphorylated by the kinase activity the affinity for microtubules decreases, consistent with observations on brain tau [27]. However, the most conspicuous effect is that on the binding capacity which markedly decreases upon phosphorylation (3-fold or more), down to values typical of brain tau. This suggests that phosphorylation affects primarily the conformation of tau such that it occupies a larger area on the microtubule surface; the same effect may be related to the altered mobility on SDS gels. It is noteworthy that the phosphorylation sites are clustered in areas flanking the repeat region, i.e. in the middle of the molecule and in the C-terminal tail (Fig. 3). While the strength of the microtubule binding is mainly determined by the repeats, each of the flanking regions contributes a moderate additional increase in affinity ( $-1.5$  kcal/mole, [6]), suggesting that the fine-tuning of tau's assembly onto microtubules is achieved via phosphorylation of the weakly binding flanking regions.

These data are a direct demonstration that the Alzheimer-like phosphorylation of tau leads to a reduction in microtubule binding. In the cell this would lead to a destabilization of microtubules and hence to a loss in axonal transport, since microtubules provide the tracks for vesicle traffic driven by motor proteins. This might constitute a major cause for the degeneration of nerve cells.

*Acknowledgements:* We would like to thank the following colleagues for excellent technical assistance: A. Malchert and U. Böning (clon-

ing), H. Korte (peptide sequencing), R. Bretthauer and J. Müller (protein preparation and photography). We also thank Dr. B. Lichtenberg-Kraag for many discussions throughout this work. The expression vector pET was kindly provided by Dr. W.F. Studier. The project was supported by the Bundesministerium für Forschung und Technologie and the Deutsche Forschungsgemeinschaft. This study contains part of the doctoral theses of N. Gustke and B. Steiner.

## REFERENCES

- [1] Baudier, J. and Cole, R.D. (1987) *J. Biol. Chem.* **262**, 17577–17583.
- [2] Bialojan, C. and Takai, A. (1988) *Biochem. J.* **256**, 283–290.
- [3] Biernat, J., Mandelkow, E.-M., Schröter, C., Lichtenberg-Kraag, B., Steiner, B., Berling, B., Meyer, H.E., Mercken, M., Vandermeeren, A., Goedert, M. and Mandelkow, E. (1992) *EMBO J.* **11**, 1593–1597.
- [4] Braak, H. and Braak, E. (1991) *Acta Neuropath.* **82**, 239–259.
- [5] Brion, J.P., Hanger, D.P., Couck, A.M. and Anderton, B.H. (1991) *Biochem. J.* **279**, 831–836.
- [6] Butner, K.A. and Kirschner, M.W. (1991) *J. Cell Biol.* **115**, 717–730.
- [7] Cleveland, D.W., Hwo, S.-Y. and Kirschner, M.W. (1977b) *J. Mol. Biol.* **116**, 207–225.
- [8] Dedner, N., Meyer, H.E., Ashton, C. and Wildner, G.F. (1988) *FEBS Lett.* **236**, 77–82.
- [9] Ennulat, D.J., Liem, R.K.H., Hashim, G.A. and Shelanski, M.L. (1989) *J. Biol. Chem.* **264**, 5327–5330.
- [10] Geisler, N., Vandekerckhove, J. and Weber, K. (1987) *FEBS Lett.* **221**, 403–407.
- [11] Goedert, M., Wischik, C., Crowther, R., Walker, J. and Klug, A. (1988) *Proc. Natl. Acad. Sci. USA* **85**, 4051–4055.
- [12] Goedert, M., Spillantini, M., Jakes, R., Rutherford, D. and Crowther, R. (1989) *Neuron* **3**, 519–526.
- [13] Goedert, M., Sisodia, S.S. and Price, D.L. (1991) *Curr. Opin. Neurobiol.* **1**, 441–447.
- [14] Greenberg, S.G. and Davies, P. (1990) *Proc. Natl. Acad. Sci. USA* **87**, 5827–5831.
- [15] Grundke-Iqbal, I., Iqbal, K., Tung, Y., Quinlan, M., Wisniewski, H. and Binder, L. (1986) *Proc. Natl. Acad. Sci. USA* **83**, 4913–4917.
- [16] Hagedstedt, T., Lichtenberg, B., Wille, H., Mandelkow, E.-M. and Mandelkow, E. (1989) *J. Cell Biol.* **109**, 1643–1651.
- [17] Himmler, A., Drechsel, D., Kirschner, M. and Martin, D. (1989) *Mol. Cell. Biol.* **9**, 1381–1388.
- [18] Hirokawa, N., Shiomura, Y. and Okabe, S. (1988) *J. Cell Biol.* **107**, 1449–1459.
- [19] Ishiguro, K., Ihara, Y., Uchida, T. and Imahori, K. (1988) *J. Biochem.* **104**, 319–321.
- [20] Ishiguro, K., Omori, A., Sato, K., Tomizawa, K., Imahori, K. and Uchida, T. (1991) *Neurosci. Lett.* **128**, 195–198.
- [21] Kosik, K., Orecchio, L., Binder, L., Trojanowski, J., Lee, V. and Lee, G. (1988) *Neuron* **1**, 817–825.
- [22] Kosik, K. (1990) *Curr. Opin. Cell Biol.* **2**, 101–104.
- [23] Ksiazek-Reding, H. and Yen, S.H. (1991) *Neuron* **6**, 717–728.
- [24] Lee, G., Cowan, H. and Kirschner, M. (1988) *Science* **239**, 285–288.
- [25] Lee, V.M.Y., Balin, B.J., Otvos, L. and Trojanowski, J.Q. (1991) *Science* **251**, 675–678.
- [26] Lichtenberg-Kraag, B., Mandelkow, E.-M., Biernat, J., Steiner, B., Schröter, C., Gustke, N., Meyer, H.E. and Mandelkow, E. (1992) *Proc. Natl. Acad. Sci. USA*, 5384–5388.
- [27] Lindwall, G. and Cole, R.D. (1984) *J. Biol. Chem.* **259**, 5301–5305.
- [28] Mandelkow, E.-M., Herrmann, M. and Rühl, U. (1985) *J. Mol. Biol.* **185**, 311–327.
- [29] Meyer, H.E., Hoffmann-Posorske, E. and Heilmeyer, L.M.G. (1991) *Methods Enzymol.* **201**, 169–185.
- [30] Steiner, B., Mandelkow, E.-M., Biernat, J., Gustke, N., Meyer, H.E., Schmidt, B., Mieskes, G., Söling, H.D., Drechsel, D., Kirschner, M.W., Goedert, M. and Mandelkow, E. (1990) *EMBO J.* **9**, 3539–3544.
- [31] Studier, W.F., Rosenberg, A.H., Dunn, J.J. and Dubendorff, J.W. (1990) *Methods Enzymol.* **185**, 60–89.
- [32] Wood, J., Mirra, S., Pollock, N. and Binder, L. (1986) *Proc. Natl. Acad. Sci. USA* **83**, 4040–4043.
- [33] Drewes, G., Lichtenberg-Kraag, B., Döring, F., Mandelkow, E.-M., Biernat, J., Goris, J., Dörre, M. and Mandelkow, E. (1992) *EMBO J.* **11**, 2131–2138.